

Phase transitions and critical phenomena of tiny grains thin films synthesized in microwave plasma chemical vapor deposition and origin of ν_1 peak

Mubarak Ali,^{a,*} I-Nan Lin^b

^a Department of Physics, COMSATS Institute of Information Technology, Islamabad 45550, Pakistan.

^b Department of Physics, Tamkang University, Tamsui Dist., New Taipei City 25137, Taiwan (R.O.C.).

*corresponding address: mubarak74@comsats.edu.pk, mubarak74@mail.com , Ph. +92-51-90495406

Abstract- Different trends have been observed in Raman analyses and electron field emission measurements of ultrananocrystalline diamond (UNCD) and nanocrystalline diamond (NCD) films synthesized in plasma-based chemical vapor deposition techniques. Phase transitions in any material are crucial as they may be the origin of new phenomenon. In the present work, it has been observed that dynamics determine the structure of tiny grains of UNCD and NCD films and those made in two-dimensional structure they stretched in the direction of impinging electron streams where diffusion of electrons states of atoms is orientation based. In those tiny grains where atoms stretch less photons of hard X-ray still retain two-dimensional structure where atoms are more like in oval shape, on stretching one-dimensionally. On the other hand, those tiny grains where all atoms are stretched more (one-dimensionally and uniformly), on propagation of photons on surfaces of their electronic structures, they are transformed into grating like shapes. In Raman spectra, peaks related to ν_1 band and D* band are due to those tiny grains of UNCD and NCD films which are

transformed into grating like shapes and two-dimensional structures, respectively. Field emission characteristics of UNCD and NCD films are resulted on the basis of tiny grains transformed into grating like shapes. High resolution transmission electron microscopy analyses physically show transforming of two different structures of tiny grains in so called UNCD and NCD films and validate the observations.

Keywords: Tiny grains; Dynamics; Phase transitions; Raman spectra; Field emission

Introduction:

Development of materials in tiny size and investigating their characteristics at nanoscale level requires a new sort of observations. Where dynamics influence the process at nanometric level, phase transitions of a material (at nanoscale) may be considered, thus, pronounced and different effects may result from such materials. Large number of publications has appeared on fabrication of ultrananocrystalline diamond (UNCD) and nanocrystalline diamond (NCD) films under varying conditions and their synthesis methods mainly involve plasma-assisted chemical vapor deposition (CVD) techniques. Performances of these UNCD/NCD films are mainly addressed in terms of grains sizes, their distributions, binding energies of different phases and features of Raman peaks. In microwave plasma enhanced CVD (MPE-CVD), tiny grains of UNCD/NCD films may be formed under the attained dynamics of individual carbon atoms operating in nanometric range before their agglomeration followed by their deposit in thin film under the emerged dynamics and the localized dynamics may influence the atoms' amalgamation at large under slightly varied process conditions. In non-equilibrium system, such as MPCVD process, carbon atoms and their made tiny grains are expected to heat locally. Those atoms amalgamated in monolayer tiny grain under the same rate of dynamics they may stretch one-dimensionally in the direction of impinging electron streams (orientation-based diffusion of electron states of carbon atoms under uniformly transferred kinetic energy of striking electron streams of plasma) or they may deform depending on the mechanisms of striking electron streams/electrons (non-orientation-based diffusion of electron states of carbon atoms under non-uniformly transferred kinetic energy of striking electron streams

electrons) as electron streams/electrons are everywhere in plasma contaminated environment of reactor. Again, photons are plentiful in microwave plasma contaminated environment and their propagation on the surfaces of such electronic structures (of tiny grains) may modify the structures under the fixed amount of energy. In the published work on UNCD/NCD films reveals more or less stretching of tiny grains in HR-TEM images (and also deformation of carbon atoms in tiny grains) and it is hard to recognize most of the atoms in their spherical shapes. Principally, such tiny grains should deal with different phases (instead of diamond phase) depending on the attained dynamics of individual atoms while amalgamating followed by electron dynamics of atoms while binding under their localized heating. These provide strong incentive to discuss dynamics of amalgamating atoms (into tiny grains) along with their agglomeration of tiny grains in thin film, deformation and one-dimensional stretching of atoms of tiny grains under specific process conditions followed by the characteristics and performance's investigation of those films.

In the present work, different UNCD/NCD films were synthesized in MPE-CVD system, amalgamation of carbon atoms and phase transitions of their tiny grains were investigated with relevance to localized dynamics. Phase transitions of tiny grains in terms of Raman spectra and field emission characteristics are studied in detail. Confusion has been going on since three decades regarding the origin of peak related to ' ν_1 band' in Raman spectra and it was considered to be due to the size of the grains or the presence of transpolyacetylene layers around tiny grains. Present study shows different one-dimensional stretching and deformation of tiny grains and indicates the real reason of peak related to ' ν_1 band' along with critical phenomena of tiny grains under which localized surface plasmons is disregarded.

Experimental details:

To synthesize so called UNCD/NCD films, microwave plasma enhanced chemical vapor deposition (MPE-CVD) system (IPLAS-Cyrannus, 2.45 GHz) was utilized. A schematic of the MPE-CVD set up have been shown in previously published work [1]. N-type Si wafers (resistivity: 1-5 Ohm-cm) were used as substrate material. Nucleation duration was set to 30 minutes in each experiment,

whereas, deposition time was 60 minutes. Prior to loading the samples in the chamber, substrates were cleaned by ultrasonic agitation for the duration of 30 minutes in methanol solution containing nanodiamond powders of 30 nm and titanium powders of 325 mesh to generate nucleation sites. The total mass flow rate was 200 sccm and was kept constant in each experiment. The substrate temperature was measured by K-type thermocouple and was $700^{\circ}\text{C}\pm 10^{\circ}\text{C}$ in UNCD/NCD films synthesized with 6 % H_2 in argon –rich methane mixture, whereas, the temperature was significantly lowered to $500^{\circ}\text{C}\pm 10^{\circ}\text{C}$ in UNCD/NCD films which were synthesized without H_2 . On increasing chamber pressure from 100 torr to 200 torr at constant microwave power (1400 watts) no remarkable difference in temperature was noted. Due to lower thermal conductivity of Ar than H_2 , heating of substrate by plasma is greatly reduced in Ar-rich CH_4 mixture [2]. Surface morphologies of various UNCD/NCD films were analyzed by Field Emission Scanning Electron Microscope (FE-SEM, ZEISS, Model: SIGMA). Peaks related to various phases were analyzed by Raman spectroscopy (Renishaw; 325 nm and HR800 UV; 632.8 nm). Electron field emission (EFE) measurements of UNCD/NCD films were made by using a tunable parallel plate set-up and $I - V$ characteristics were measured by an electrometer (Keithley 237) under vacuum level of 10^{-6} torr. Dark field, bright field, high resolution images and SAED patterns of various UNCD/NCD films were taken by HR-TEM (JEOL JEM2100F) operated at 200 kV. Photon energy of different bands in UNCD/NCD films were deduced by core loss and low loss EELS. Plasma species formed in microwave chamber were detected *in-situ* by Optical Electron Spectroscopy (B&WTEK BTC 112E) in the range of 200 – 1050 nm.

Results and discussion:

Surface morphologies of so called UNCD/NCD films synthesized at various chamber pressures are shown in Figures S1 (a) to S1 (c); at 150 torr more tiny grains are in needle-like shapes. In UNCD/NCD films synthesized at 100 torr and 200 torr, more tiny grains are in spherical-like shapes. Morphological features of tiny grains in film synthesized without H_2 gas (Figure S2) are almost similar to the morphological features of tiny grains in film synthesized at 6 % H_2 (Figure

S1b). Raman spectra of different films synthesized at 100 torr, 150 torr and 200 torr are shown in Figure 1 (a) indicating different intensity levels of peaks related to ' ν_1 band'. The ' ν_1 band' is more pronounced in films synthesized at 100 torr and 200 torr compared to the film synthesized at 150 torr. On the other hand, the ' ν_1 band' is intensive in film synthesized without H₂ gas (Figure S3) compared to the films synthesized at 6% H₂ (Figure 1a). Field emission current density as a function of applied field at various chamber pressures is shown in Figure 1 (b). Film synthesized at 100 torr shows superior EFE properties where 'turn on field' is 11.52 V/ μ M (the lowest value) and the large EFE current density (> 2.0 mA/cm²). The 'turn on field' is the highest (25 V/ μ M) in the film synthesized at 150 torr, whereas, it is recorded 16.4 V/ μ M at 200 torr. Field emission current density as a function of applied field in different UNCD/NCD films synthesized without H₂ and with H₂ (3% and 6%) in Ar-rich CH₄ mixture are shown in Figures S4 (a-c). In Figures S4 (a) to S4 (c), the general trend of the 'turn on field' is more morphology-dependent; the value of 'turn on field' at 100 torr is lower than that at 150 torr (same trend is noted in Figure 1b). Under lower chamber pressure (at 100 torr), impingement of electron streams to tiny grains are highly effective and they are stretched uniformly, whereas, the large value of 'turn on field' in film synthesized at 200 torr (Figure S4a) was due to less stretching of tiny grains as the impinging electron streams are less effective at higher chamber pressure (200 torr) and detailed discussions of those phenomena will be given in the following sections.

Dark field TEM images of UNCD/NCD film synthesized at 100 torr and 200 torr are shown in Figures S5 (a) and S6 (a) where smaller dark spots are related to isolated tiny grains and bigger dark spots are related to coalesced tiny grains and their contrast is more visible in bright field TEM images (Figures S5b and S6b); in some regions of the film tiny grains amalgamated and in some regions dispersed. SAED patterns of the same regions of films are shown in Figures S5 (c) and S6 (c) where intensity spots do not show precise rings related to various planes of diamond structure.

HR-TEM image taken from the UNCD/NCD film synthesized at 100 torr is shown in Figure 2 (c) and from the figure two regions of magnified images are shown in Figures 2 (a) and 2 (b). In

Figure 2 (a), several tiny grains in two-dimensional structures are transformed into grating like shapes and are overlaid as well. However, Figure 2 (b) shows only one tiny grain transformed into grating like shape. The insert in Figure 2 (c) shows spectral analysis of the structure shown in Figure 2 (b), which also reveals grating like shape of the tiny grain. Figure S7 shows HR-TEM image taken from another region of UNCD/NCD film and highlights different features of the tiny grains transformed into grating like shapes (important portions are labelled). Gap between two grating like shapes labeled by (2) indicates formation of canal like channel which is referred as 'graphitic filament' [1, 3]. HR-TEM image taken from the UNCD/NCD film synthesized at 200 torr is shown in Figure 3 (c) and from the figure two regions of magnified images are shown in Figures 3 (a) and 3 (b), respectively. In Figure 3 (a), impinging electron streams for shorter period result into less stretching of tiny grain and photons emitted on the interactions of charged species of plasma still retain electronic structure in two-dimensional structure while propagating on the surface; electronic shell (s) of atom is (are) nearly overlap into the next adjacent ones of one-dimensional arrays (less orientation-based diffusion of electrons states of carbon atoms). In Figure 3 (b), tiny grains are stretched more (more orientation-based diffusion of electrons states of carbon atoms) and on propagating photons of hard X-rays their electronic structures are transformed into grating like shapes. A canal-like channel is formed between two gratings and is denoted by red dotted line in Figure 3 (b). The insert in Figure 3 (c) shows spectral analysis of less stretched tiny grain of region 'a' and presents the features of nearly two-dimensional structure where intensity spots do not reveal the configuration as in the case of grating like shape (in the insert of Figure 2c).

Here, 'electronic structure' is referred to that structure where electronic shells of atoms of tiny grains stretched (deform) more or less under the influence of impinging electron streams (or exposure to hydrogenated microwave plasma environment). Under more stretching of tiny grains having two-dimensional structures their electronic structures are transformed into smooth elements. Elements and their inter-spacing in each grating like shape move parallel to each other and they possess equal widths ($\sim 0.10 \text{ nm} = 1 \text{ \AA}$) as labeled in Figures 2 (b) and 3 (b). X-ray with photon of

wavelength 0.1 nm is called hard X-ray and has energy 10 keV [4]. In fact, the lattice doesn't collectively oscillate on trapping/coupling of electromagnetic radiations and photons of plasma only modify the electronic structure of tiny grain (in two-dimensional structure) into smooth elements by transferring their energy. Where electron streams impinged normal to atoms of tiny grains, atoms do not stretch one-dimensionally and they reveal swelling and photons do not transform (modify) such tiny grains into smooth elements while propagating on the surface of their electronic structure because they don't stretch one-dimensionally. By varying the time of impinging electron streams and due to greater number of electronic shells in metallic elements we can alter the widths of elements and their inter-spacing distances in tiny metallic colloids (and their extended shapes) and we extensively studied the phenomenon in gold and silver [5-9]. Further details of one-dimensional stretching of tiny grains and deformation are given elsewhere [10].

Core loss EELS of UNCD/NCD films at the same regions from where HR-TEM images were taken are shown in Figures S8 (a) and (b). In Figures S8 (a) and (b) regions of both the films synthesized at 100 torr and 200 torr show an abrupt rise near 292 eV (σ^* -band) and a large dip in the vicinity of 305 eV, which is referred to as the nature of diamond [11, 12]. In Figures S8 (a) and (b), both spectra show hump-like peaks at 328 eV. However, due to transformation of more tiny grains into grating like shapes, the peak is more pronounced in film synthesized at 100 torr. In low loss EELS, graphitic phase shows a prominent peak at s_3 (27 eV), whereas, the a-C phase shows a peak at s_1 (22 eV) [12, 13], however, in Figure S9 (a) the peak at 27 eV is not present in film synthesized at 100 torr and it is not exactly at 22 eV in film synthesized at 200 torr [Figure S9 (b)], which indicate different rate of stretching of tiny grains in two different UNCD/NCD films. In Figure S9 (a), hump-like peak with maximum height at 65 eV is an indication of greater number of tiny grains, which are stretched more and their electronic structures are transformed into grating like shapes and this is in accordance to EFE measurement and HR-TEM investigations.

In Raman spectroscopy of UNCD/NCD films, the peak at 1150 cm^{-1} has been attributed to nanocrystalline diamond [13-15], however, the ν_1 peak (at 1150 cm^{-1}) cannot originate from a

nanodiamond or related sp^3 -bonded phase but assigned to transpolyacetylene segments at grain boundaries and surfaces [16]. Nemanich *et al.* [14, 15] proposed that 1150 cm^{-1} peak arises from nanocrystalline or amorphous diamond. In the Raman spectroscopy of UNCD/NCD film, the sharp peak at 1332.1 cm^{-1} is the characteristic of diamond and broadening of the peak is related to the NCD grains [17]. In UNCD/NCD films, the peak at 1150 cm^{-1} appears hypothetically due to CH bonds and is always linked to another peak at 1450 cm^{-1} , and the peaks at 1330 cm^{-1} and 1560 cm^{-1} are due to D- band and G-band [18]. However, in the light of presented results of UNCD films, argon gas increases the rate of re-nucleation and the amount of tiny grains sizes $< 10\text{ nm}$ is enhanced significantly, also in NCD film more tiny grains have size $> 10\text{ nm}$ and depending on how many tiny grains are transformed (modified) structures into grating like shapes experienced excitations on exposure to Raman laser, from this the contributions are in the form of peak and appear at wave number 1150 cm^{-1} . In microcrystalline diamond films, the size of grain is very large and atoms are more in tetrahedron structure, accordingly, information put forth by Raman spectrum doesn't show any peak at 1150 cm^{-1} . Thus, the peak in UNCD/NCD films at wave number 1150 cm^{-1} is associated to those tiny grains transformed into grating like shapes and depending on their quantity excitations levels are altered followed by the variation in the intensity of ' ν_1 peak'; different intensities of ' ν_1 band' are related to the number of the tiny grains transformed into grating like shapes. Now, those tiny grains, which are transformed into grating like shapes, electronic excitations are executed at higher energy comparatively to both tetrahedron and disordered structures of the film, thus, ' ν_1 peak' is originated at wave number 1150 cm^{-1} . Prior to transforming tiny grains into grating like shape, they were in two-dimensional structure and according to fundamental of materials science, the packing factor of such structure is greater than tetrahedron structure. Obviously, the peak at wave number $\sim 1150\text{ cm}^{-1}$ is linked to greater packing factor of the grating like structure. Due to lower packing factor of the diamond structure, the peak is recorded at wave number 1332 cm^{-1} . Briefly, on exposure of Raman laser to the film, Raman signals recorded intensities depending on the energy of phase, thus, peaks are originated at different wave numbers,

that is, more the energy of phase less is the wavelength of peak (and higher is the wave number). In the Raman spectrum, the positions of peaks of different carbon phases is in accordance to the Planks' equation of energy –wavelength. Thus, we conclude that 'ν₁ band' is not due to size of tiny grain itself or layer of transpolyacetylene present around them but is related to electronic excitations in the tiny grains, which are transformed (modified) into grating like shapes. Incorporating H₂ in Ar-rich CH₄ mixture either eliminates the 'ν₁ band' or it appears with less intensity. Without addition of H₂ in Ar-rich CH₄ mixture, peak related to 'ν₁ band' becomes pronounced (Figure S3). On varying concentrations of gases, the nature of tiny grains both in terms of physics and chemistry is altered and UNCD/NCD films count different numbers of tiny grains, which are transformed into grating like shapes and this turns into different intensities of 'ν₁ band'; on penetrating different wavelengths of Raman signals in UNCD/NCD films different intensities of 'ν₁ band' are discernable [19, 20]. Optical Emission Spectra taken at various chamber pressures is in accordance to Raman spectroscopy of UNCD/NCD films (Figure S10) where peak related to H₂ gas was absent in the film synthesized without H₂ gas and indicates the stabilization of plasma through atomic hydrogen, which was resulted on disassociating CH₄. Optical Emission Spectra (OES) taken at various chamber pressures are shown in Figure S10 where the same trend of emission intensities of CH and C2 was observed. OES collected for 10 seconds in each experiment with regular intervals and revealed the same results in terms of emission intensities of CH and C2 (Figure S10). For films synthesized without hydrogen, hydrogen species are not present in OES and there was very little amount of hydrogen involved in the process of C-H formation (during the growth of UNCD/NCD films) and support the results of Raman spectroscopy. At zero % H₂, the source of small amount of hydrogen was the CH₄, which dissociate in microwave chamber as the result of microwave power. Collisions of energetic argon species facilitate the dissociation of CH₄ [21]. As shown in Figure S10, the nature of plasma changed in the chemical reactor; up to 20 torr pressure, high intensity peaks of Ar-I are present. As the chamber pressure exceed, high intensity peaks of C2 radicals is appeared while Ar peaks is disappeared. An earlier in-situ OES study of Ar-rich microwave plasma

shows similar type of Ar emission over wavelength 700 nm [22]. In the absence of H₂ gas, it is believed that some hydrogen atoms come from the disassociation of CH₄ and assist plasma to be stabilized [23]. As a result of microwave power, argon atoms are excited and dissociate CH₄ molecules for their activation [20]. OES of processing plasma in microwave plasma chamber have been worked out by number of groups [24, 25], which show similar type of information as shown in Figure S10.

Impinging electron streams stretched atoms of tiny grains having two-dimensional structures in the direction of their impingement, as consequence of this, electronic shells of atoms overlapped into the next adjacent ones of each one-dimensional array. In due course of time, photons emitted through the interactions of charged particles, their propagation on the surfaces of one-dimensionally stretched electronic structure of tiny grain modify them into smooth elements by utilizing their energy and through opposite wave fronts. Briefly, under the regime of dynamics those tiny grains configured two-dimensional structure they stretched uniformly in the direction of impingement of electron streams and on propagating photons they either transformed their electronic structures into two-dimensional lattices (those stretched less) or into grating like shapes (those stretched more). In out of equilibrium system, different interactions contributed to induce electronic/ionic temperatures [26]. Ye *et al.* [27] predicted the local temperature of a system out of equilibrium. A schematic presentation of tiny grain where atoms are configured into compact monolayer two-dimensional structure (25 atoms) is shown in Figure 4 (a). Impinging electron streams for less or more time stretched tiny grain in the direction of their impingement; less stretched electronic structure of tiny grain is shown in Figure 4 (b) while more stretched electronic structure of tiny grain is shown in Figure 4 (c). In less stretched electronic structure of tiny grain atoms are in their slightly deformed shapes like oval (Figure 4d), whereas, in more stretched tiny grain photons transformed (modified) electronic structure into smooth elements (Figure 4e). Photons emit due to de-excitations of excited states of electrons in carbon atoms are different to those emitted on interacting gaseous plasma species. The photons emitted in atoms of elements having valency shell (while heating locally) are

utilized to bind their atoms, whereas, the photons emitted on losing shells of inert gases (while in the state of plasma) are utilized to modify the electronic structures of tiny grains.

Conclusions:

Tiny grains of carbon atoms evolve structure at nanoscale depend on the attained dynamics of their individual atoms at the instant of amalgamation. Binding of amalgamated atoms (of tiny grains) is under the process of photon coupling where one atom emits photon under de-excited state at suitable level of heating locally, which is absorbed by nearby atoms to go into its excited state. Thus, in electron dynamics atoms bind permanently in the lattice of tiny grain. The size of tiny grain depends on both localized conditions of the process as well as overall conditions of the process. Such tiny grains go through various deformations and one-dimensional stretching depending on their interactions to plasma contaminated environment. Thus, agglomeration of tiny grains into thin film is under their emerged dynamics. In microwave plasma chemical vapour deposition environment, discernible phase of two dominant structures of tiny grains in UNCD/NCD films have been observed. A tiny grain in two-dimensional structure is made through atom-to-atom amalgamation under the attained dynamics while heating locally. Such tiny grains stretch more or less in the direction of impingement of electron streams depending on the time of impinging electron streams and those stretched less propagating photons on their surfaces still retain them into two-dimensional structure where atoms are in oval shape, whereas, those tiny grains stretched more propagating photons on the surfaces of their electronic structures transform (alter or modify) them into grating like shapes where electronic shells of atoms overlapped into the next adjacent ones of one-dimensional arrays (orientation-based diffusion of electrons states of atoms). This process of overlapping of electronic shells of atoms into the next adjacent ones of one-dimensionally stretched arrays in the direction of impingement and propagating photons on the surfaces of electronic structures to modify their structures into smooth elements disregard the phenomenon of localized surface plasmons. In Raman spectrum, tiny grains in grating like shapes are the origin of ' ν_1 peak', whereas, those tiny grains still retaining their two-dimensional structures may be the origin of D*

peak. These phase transitions of tiny grains are critical phenomena in determining the overall performance of various UNCD/NCD films and play crucial role in evaluating the performance of films for various applications. The lower ‘turn on field’ of UNCD/NCD film is due to transformation of more tiny grains into grating like shapes. HR-TEM images of tiny grains in UNCD/NCD films reveal different mechanisms of their transformation; in some regions they assemble tip-to-tip and extend in size, in some regions their assembling display different orientations, in other regions they leave very small distance between each other and non-regular surfaces appear (so called ‘grain boundaries’), while in some regions there are broad distances and leave wide gaps, in some regions overlay and coalesce with non-uniform stretching of their atoms. In fact, all those phenomena contribute into the measurement of the performance of UNCD/NCD films and the most influential factor is related to those tiny grains transformed into grating like shapes. These also indicate the vital but critical role of dynamics in synthesizing thin films of so-called UNCD/NCD. Thus, characteristics of different UNCD/NCD films in term of electron field emission are not merely due to electron affinity, thermal behavior of phases, doping and charge transfer. In line with this, present studies set a new horizon in synthesizing, analyzing and evaluating the materials at nanoscale, and solicit reinvestigation of materials’ performances both in existing and future applications.

Acknowledgements:

Mubarak Ali thanks National Science Council (now MOST) Taiwan (R.O.C.) for awarding postdoctorship: NSC-102-2811-M-032-008 (2013-2014). Authors wish to thank Mr. Tsung-Min Chen for assisting films’ synthesis and Mr. Chien-Jui Yeh in TEM operation. Mubarak Ali greatly appreciates useful suggestions of Dr. M. Ashraf Atta and Dr. Abdul Waheed (CIIT, advisors).

References:

- [1] A. Saravanan, B. R. Huang, K. J. Sankaran, G. Keiser, J. Kurian, N. H. Tai, I. N. Lin, Structural modification of nanocrystalline diamond films via positive/negative bias enhanced

- nucleation and growth processes for improving their electron field emission properties, *J. Appl. Phys.* 117 (2015) 215307-11.
- [2] X. Xiao, J. Birrell, J. E. Gerbi, O. Auciello, J. A. Carlisle, Low temperature growth of ultrananocrystalline diamond, *J. Appl. Phys.* 96 (2004) 2232-2239.
- [3] S. C. Lin, C. -J. Yeh, C. L. Dong, H. Niu, J. Kurian, K. -C. Leou, I -N. Lin, The microstructural evolution of ultrananocrystalline diamond films due to P ion implantation and annealing process-dosage effect, *Diam. Relat. Mater.* 54 (2015) 47-54.
- [4] D. Attwood, *Soft X-rays and extreme ultraviolet radiation (Principles and Applications)*. Cambridge University Press, pp. 1-2 (1999).
- [5] M. Ali, I -N. Lin, The effect of the Electronic Structure, Phase Transition and Localized Dynamics of Atoms in the formation of Tiny Particles of Gold, <http://arxiv.org/abs/1604.07144> (2016).
- [6] M. Ali, I -N. Lin, Geometric structure of gold tiny particles at varying precursor concentration and packing of their electronic structures into extended shapes, <http://arxiv.org/abs/1604.07508> (2016).
- [7] M. Ali, I -N. Lin, Dynamics of colloidal particles formation in processing different precursors-elastically and plastically driven electronic states of atoms in lattice, <http://arxiv.org/abs/1605.02296> (2016).
- [8] M. Ali, I -N. Lin, Controlling morphology-structure of particles *via* plastically driven geometric tiny particles and effect of photons on the structures under varying process conditions, <http://arxiv.org/abs/1605.04408> (2016).
- [9] M. Ali, I -N. Lin, Formation of tiny particles and their extended shapes – origin of physics and chemistry of materials, <http://arxiv.org/abs/1605.09123> (2016).
- [10] M. Ali, M. Ürgen, Switching dynamics of morphology-structure in chemically deposited carbon films-a new insight, <http://arxiv.org/abs/1605.00943> (2016).

- [11] D. M. Gruen, S. Liu, A. R. Krauss, X. Pan, Buckyball microwave plasmas: Fragmentation and diamond-film growth, *J. Appl. Phys.* 75 (1994) 1758-1763.
- [12] P. Kovarik, E. B. D. Bourdon, R. H. Prince, Electron-energy-loss characterization of laser-deposited *a*-C, *a*-C:H, and diamond films, *Phys. Rev. B* 48 (1993) 12123-12129.
- [13] W. A. Yarbrough, R. Messier, Current issues and problems in the chemical vapor deposition of diamond, *Science* 247 (1990) 688-696.
- [14] R. J. Nemanich, J. T. Glass, G. Lucovsky, R. E. Shroder, Raman scattering characterization of carbon bonding in diamond and diamondlike thin films, *J. Vac. Sci. Technol. A* 6 (1988) 1783-1787.
- [15] R. E. Shroder, R. J. Nemanich, J. T. Glass, Analysis of the composite structures in diamond thin films by Raman spectroscopy, *Phys. Rev. B* 41 (1990) 3738-3745.
- [16] A. C. Ferrari, J. Robertson, Origin of the 1150cm^{-1} Raman mode in nanocrystalline diamond, *Phys. Rev. B* 63 (2001) 121405-5.
- [17] I. Jiménez, M. M. García, J. M. Albella, L. J. Terminello, Orientation of graphitic planes during the bias-enhanced nucleation of diamond on silicon: An x-ray absorption near-edge study, *Appl. Phys. Lett.* 73 (1998) 2911-2913.
- [18] J. Birrell, J. E. Gerbi, O. Auciello, J. M. Gibson, J. Johnson, J. A. Carlisle, Interpretation of the Raman spectra of ultrananocrystalline diamond, *Diam. Relat. Mater.* 14 (2005) 86-92.
- [19] R. Haubner, M. Rudigier, Raman characterisation of diamond coatings using different laser wavelengths, *Physics Procedia* 46 (2013) 71-78.
- [20] S. C. Ray, I -N. Lin, Ferroelectric behaviours of ultra-nano-crystalline diamond thin films, *Surf. Coat. Technol.* 271 (2015) 247-250.
- [21] S. J. Askari, F. Lu, Characteristics of a well-adherent nanocrystalline diamond thin film grown on titanium in Ar/CH₄ microwave CVD plasma, *Vacuum* 82 (2008) 673-677.
- [22] C. -R. Lin, *et al.*, Fabrication of highly transparent ultrananocrystalline diamond films from focused microwave plasma jets, *Surf. Coat. Technol.* 231 (2013) 594-598.

- [23] P. W. May, Y. A. Mankelevich, From Ultrananocrystalline Diamond to Single Crystal Diamond Growth in Hot Filament and Microwave Plasma-Enhanced CVD Reactors: a Unified Model for Growth Rates and Grain Sizes, *J. Phys. Chem. C* 112 (2008) 12432-12441.
- [24] Y. -C. Chu, et al., Systematic studies of the nucleation and growth of ultrananocrystalline diamond film on silicon substrates coated with a tungsten layer, *J. Appl. Phys.* 111 (2012) 124328-36.
- [25] J. -H. Jiang, Y. Tzeng, Mechanisms of suppressing secondary nucleation for low-power and low temperature microwave plasma self-bias-enhanced growth of diamond films in argon diluted methane, *AIP Advances* 1 (2011) 042117-11.
- [26] M. D. Ventra, *Electrical Transport in Nanoscale Systems* (Cambridge University Press, Cambridge, 2008).
- [27] L. Ye, D. Hou, X. Zheng, Y. Yan, M. D. Ventra, Local temperatures of strongly-correlated quantum dots out of equilibrium, *Phys. Rev. B* 91 (2015) 205106-8.

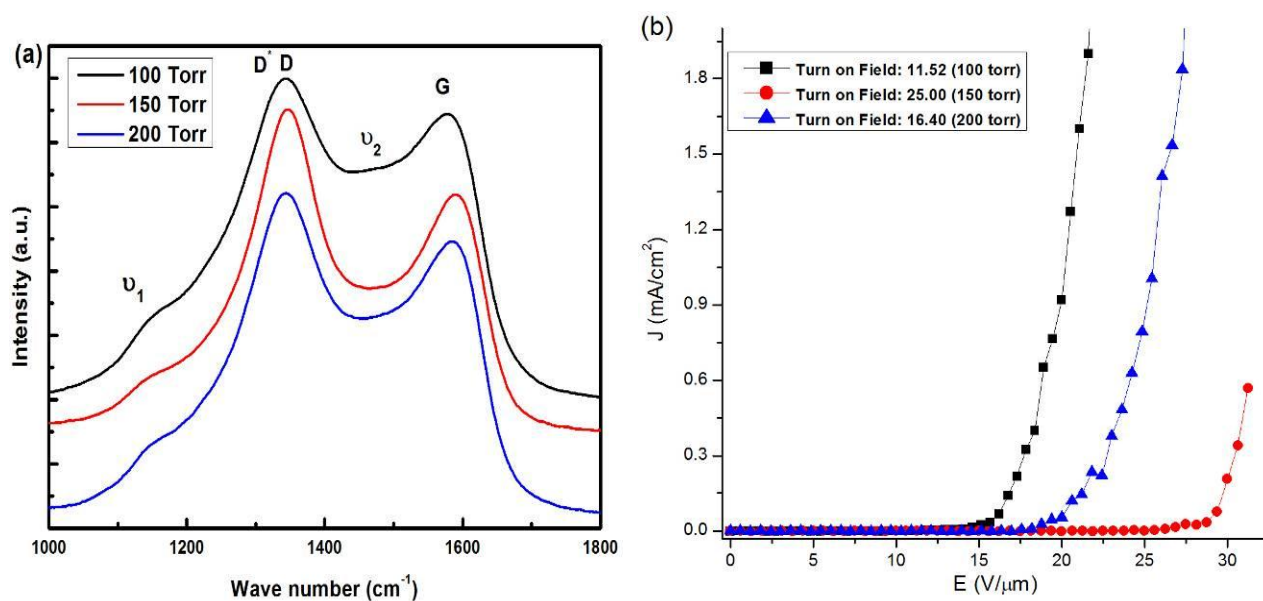


Figure 1: (a) Raman spectra and (b) electron field emission current density as a function of applied field of UNCD/NCD films synthesized at chamber pressure 100 torr, 150 torr and 200 torr; total mass flow rate: 200 sccm (6% H₂, 1 % CH₄ and 93 % argon, Ar: CH₄: H₂ = 186:2:12), microwave power: 1400 watts and deposition time: 60 minutes

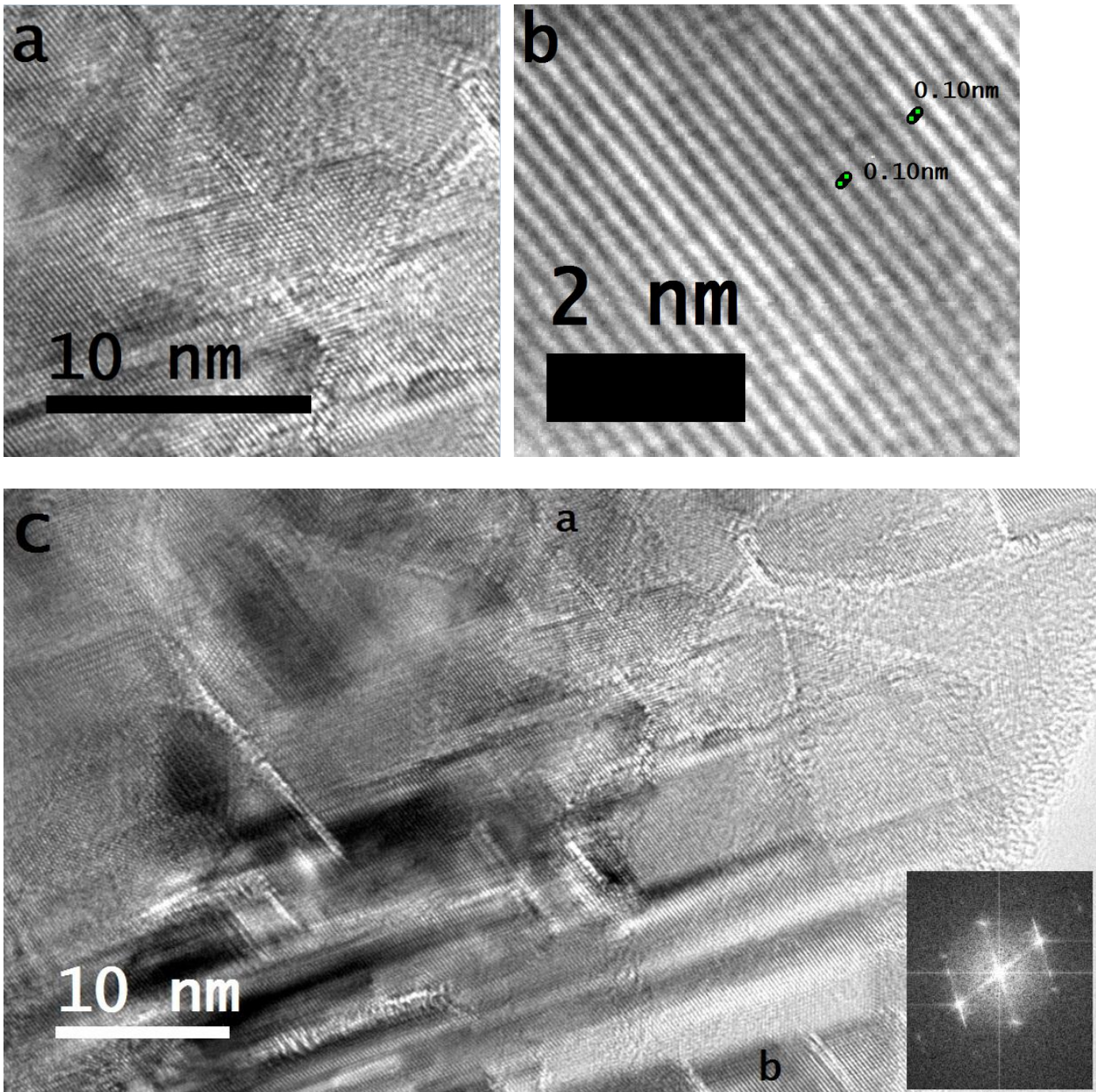


Figure 2: (a) Magnified region of HR-TEM image shows overlaying of grating like shapes, (b) magnified region of HR-TEM image shows grating like shape and (c) standard HR-TEM image shows large number of tiny grains transformed into grating like shapes; UNCD/NCD film synthesized at chamber pressure: 100 torr, mass flow rate: 200 sccm (6% H₂, 1 % CH₄ and 93 % argon), microwave power: 1400 watts and deposition time: 60 minutes.

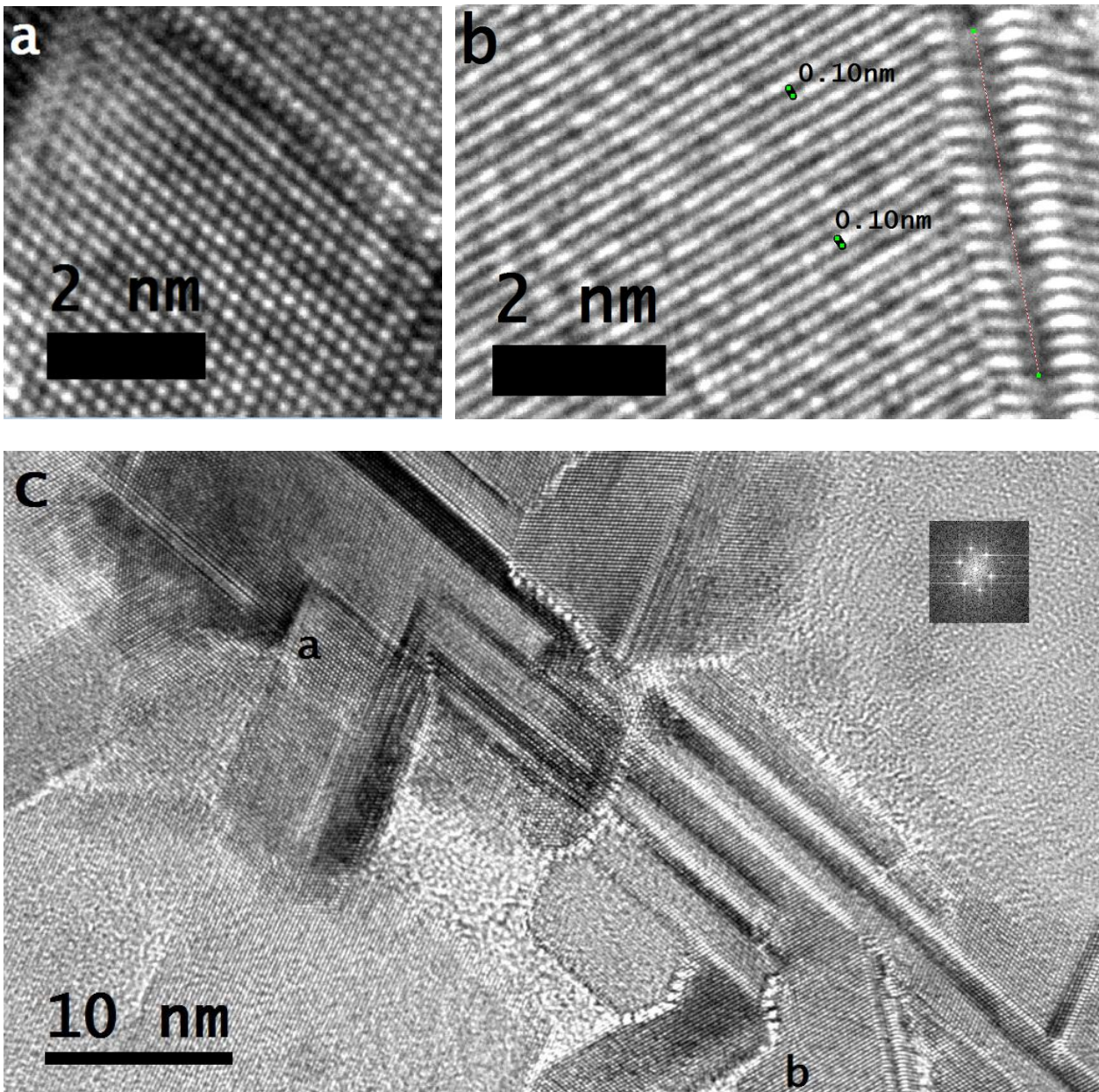


Figure 3: (a) Magnified region of HR-TEM image shows two-dimensional lattice, (b) magnified region of HR-TEM image shows grating like shape and (c) standard HR-TEM image shows several tiny grains retained two-dimensional structures and grating like shapes as well (insert shows spectral analysis of region 'a'); UNCD/NCD film synthesized at chamber pressure: 200 torr, mass flow rate: 200 sccm (6% H₂, 1 % CH₄ and 93 % argon), microwave power: 1400 watts and deposition time: 60 minutes.

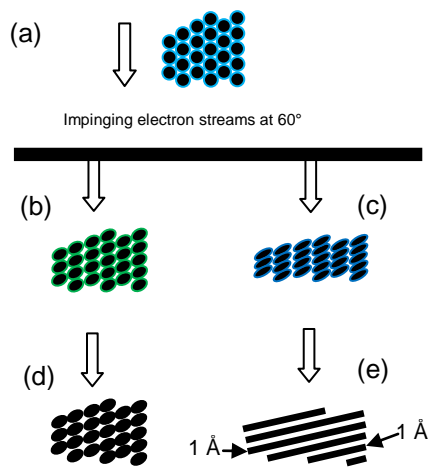
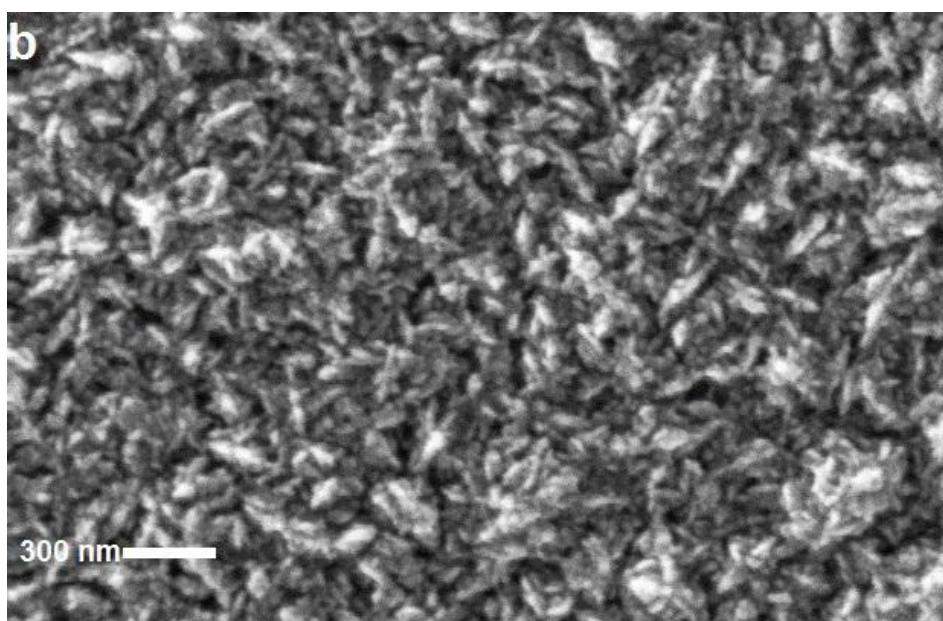
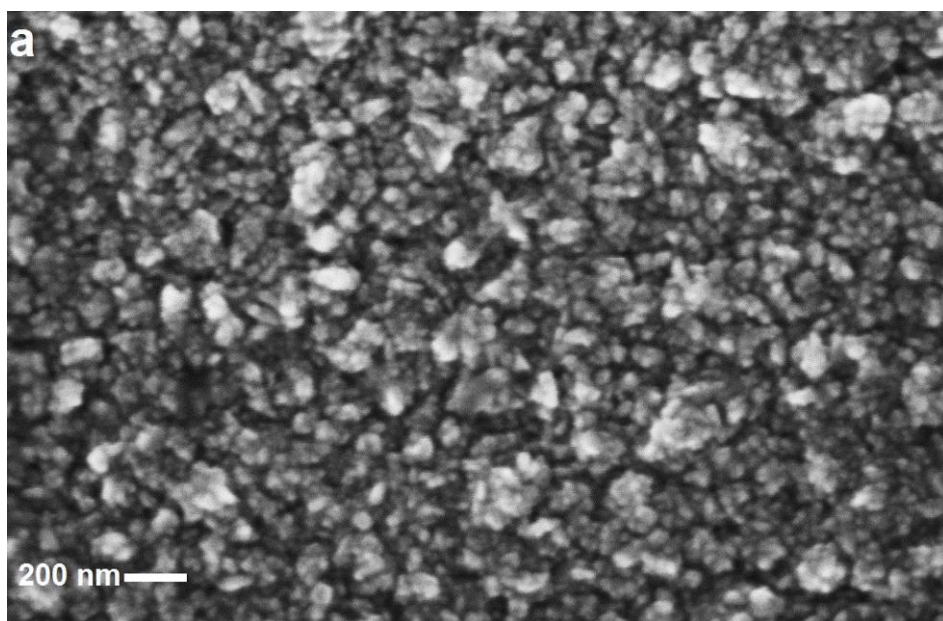


Figure 4: (a) Tiny grain in compact monolayer two-dimensional structure, on impinging electron streams at 60° to tiny grain it (b) stretched less (c) stretched more (in both cases one-dimensionally at 60°), (d) propagating photons on the surface of less stretched electronic structure (of tiny grain) modified it in two-dimensional structure but each atom is in oval-shaped and (e) propagating photons on the surface of more stretched electronic structure (of tiny grain) modified it into smooth elements (grating like shape).

Supplementary Materials



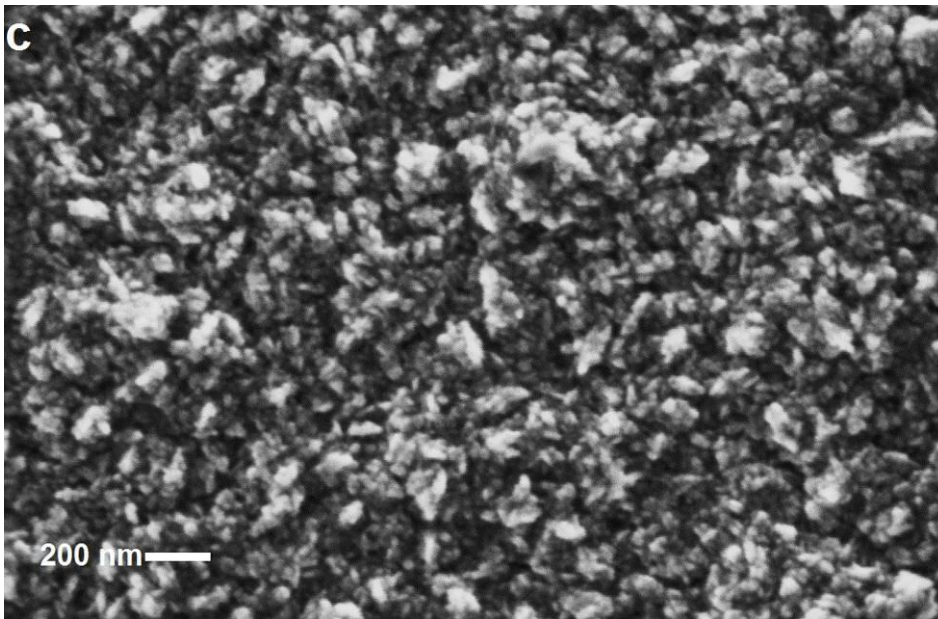


Figure S1: Surface morphologies of UNCD/NCD films synthesized at chamber pressure (a) 100 torr, (b) 150 torr, and (c) 200 torr; total mass flow rate: 200 sccm (6% H₂, 1 % CH₄ and 93 % argon, Ar: CH₄: H₂ = 186:2:12), microwave power: 1400 watts and deposition time: 60 minutes.

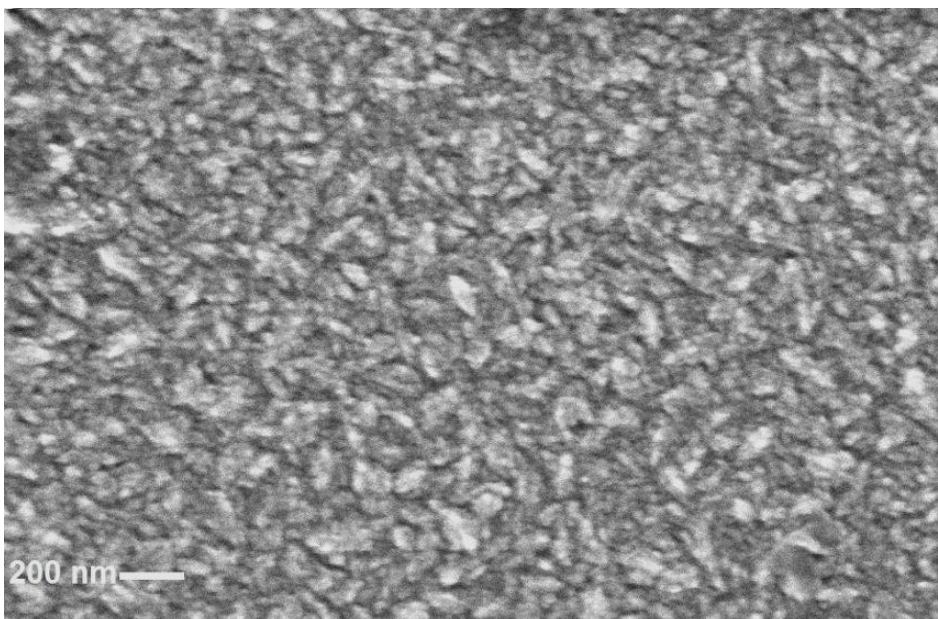


Figure S2: Surface morphology of UNCD/NCD film synthesized at chamber pressure 150 torr; total mass flow rate: 200 sccm (0% H₂, 2 % CH₄ and 98 % argon, Ar: CH₄: H₂ = 196:4:0), microwave power: 1100 watts and deposition time: 60 minutes.

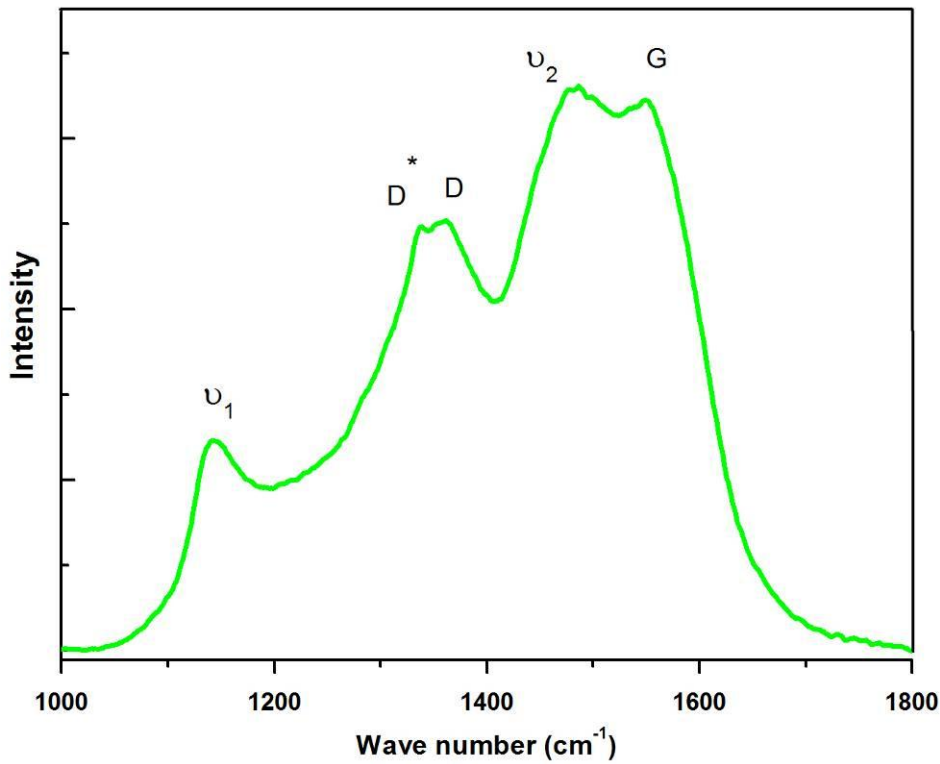
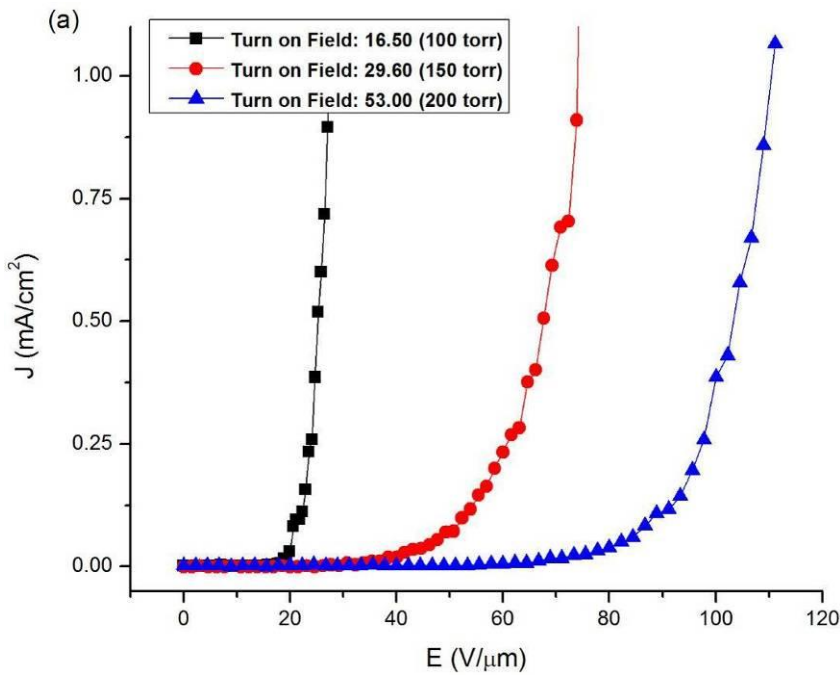


Figure S3: Raman spectrum of UNCD/NCD film synthesized at chamber pressure 150 torr; total mass flow rate: 200 sccm (0% H_2 , 2 % CH_4 and 98 % argon, Ar: CH_4 : H_2 = 196:4:0), microwave power: 1100 watts and deposition time: 60 minutes (ν_1 : $\sim 1145 \text{ cm}^{-1}$, D^* : $\sim 1310 \text{ cm}^{-1}$, D : 1332 cm^{-1} , ν_2 : $\sim 1480 \text{ cm}^{-1}$, G : $\sim 1580 \text{ cm}^{-1}$).



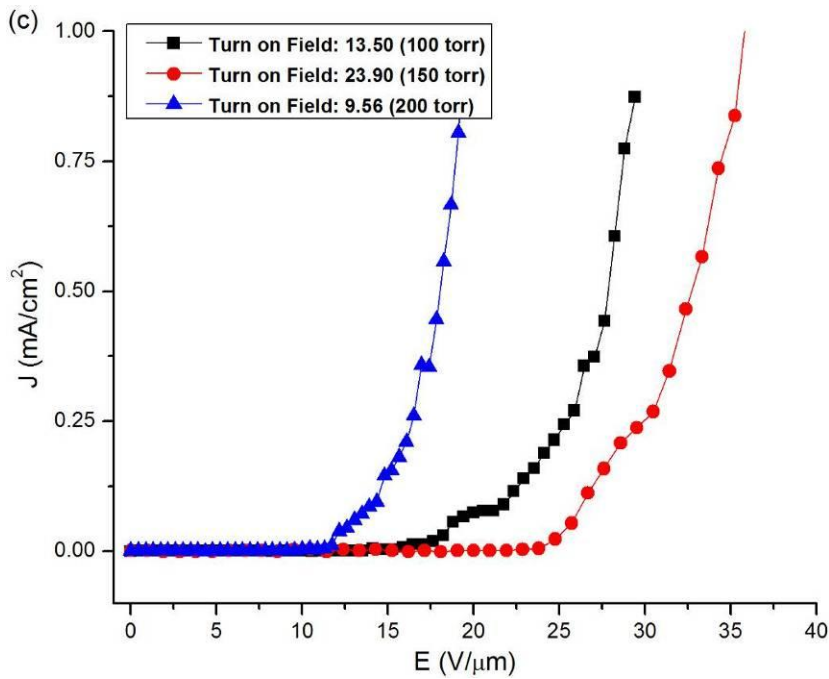
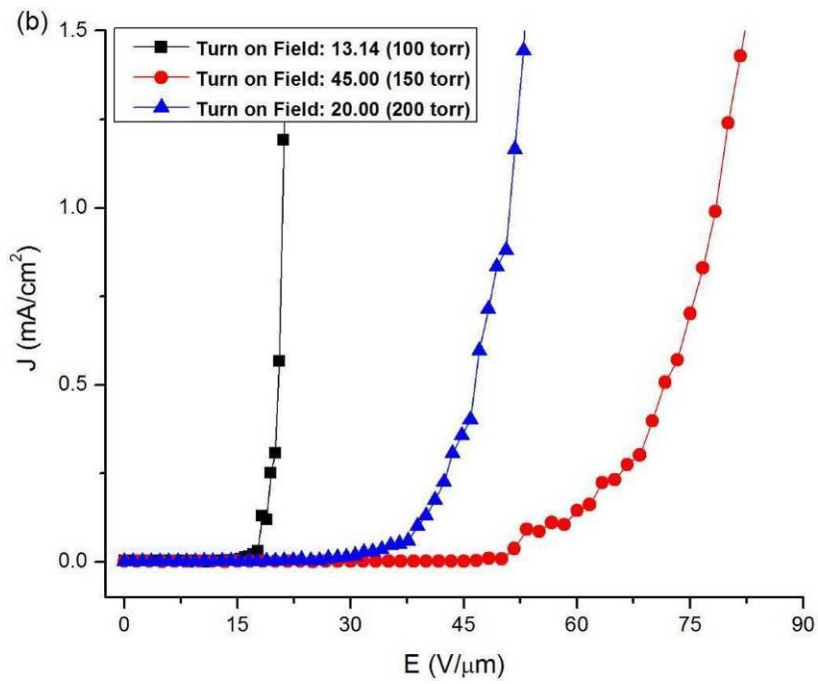


Figure S4: Electron field emission current density as a function of applied field of UNCD/NCD films synthesized at (a) without H₂, (b) 3 % H₂ and (c) 6 % H₂; 1 % CH₄, total mass flow rate: 200 sccm, microwave power: 1200 watts and deposition time: 60 minutes.

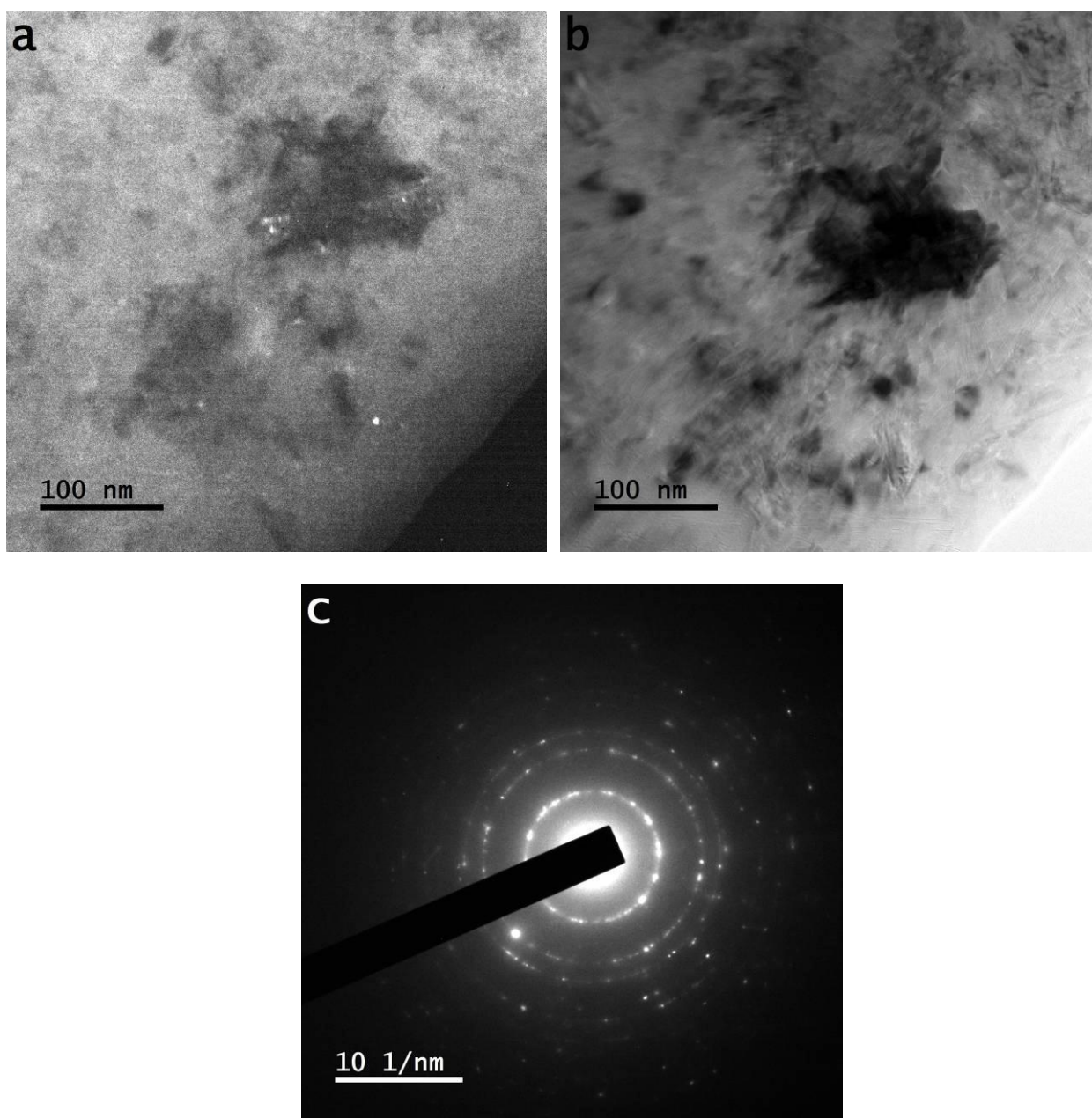


Figure S5: (a) Dark field TEM image (b) Bright field TEM image and (c) SAED pattern of UNCD/NCD film synthesized at chamber pressure: 100 torr, total mass flow rate: 200 sccm (6% H₂, 1 % CH₄ and 93 % argon), microwave power: 1400 watts and deposition time: 60 minutes.

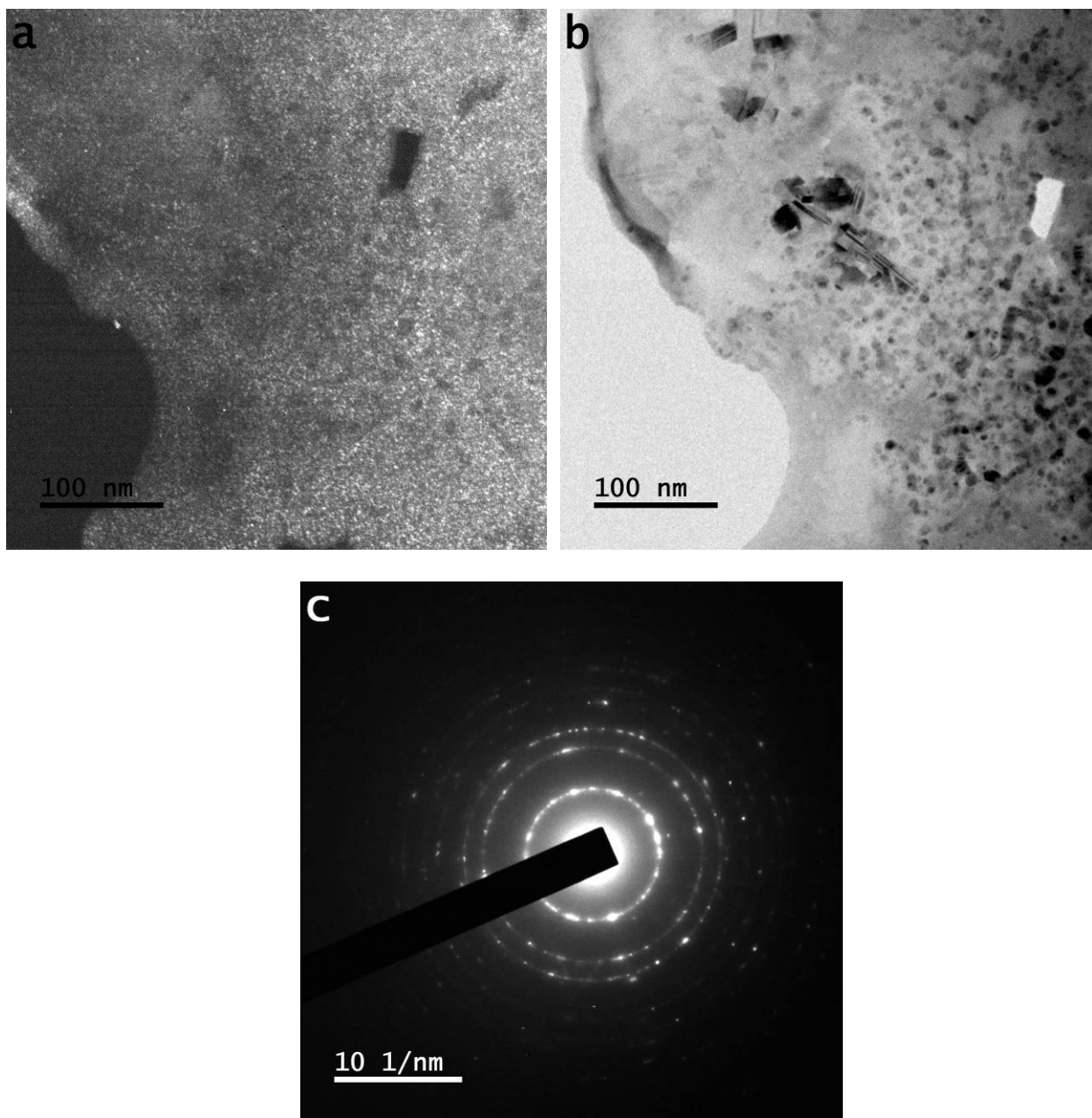


Figure S6: (a) Dark field TEM image (b) Bright field TEM image and (c) SAED pattern of UNCD/NCD film synthesized at chamber pressure: 200 torr, total mass flow rate: 200 sccm (6% H₂, 1 % CH₄ and 93 % argon), microwave power: 1400 watts and deposition time: 60 minutes.

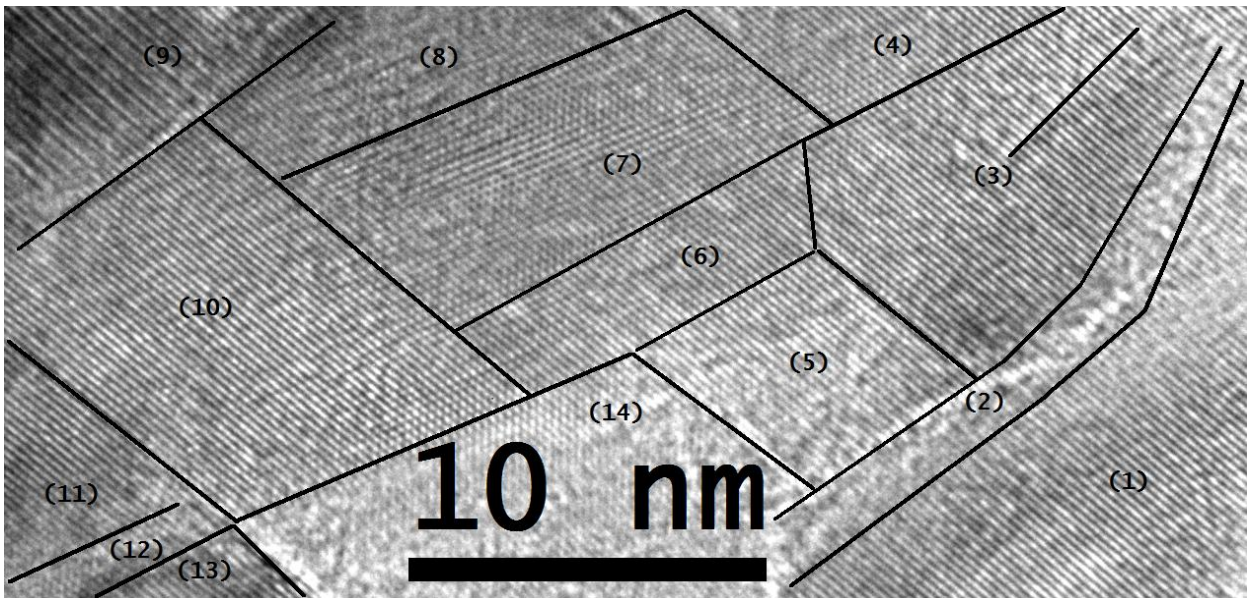
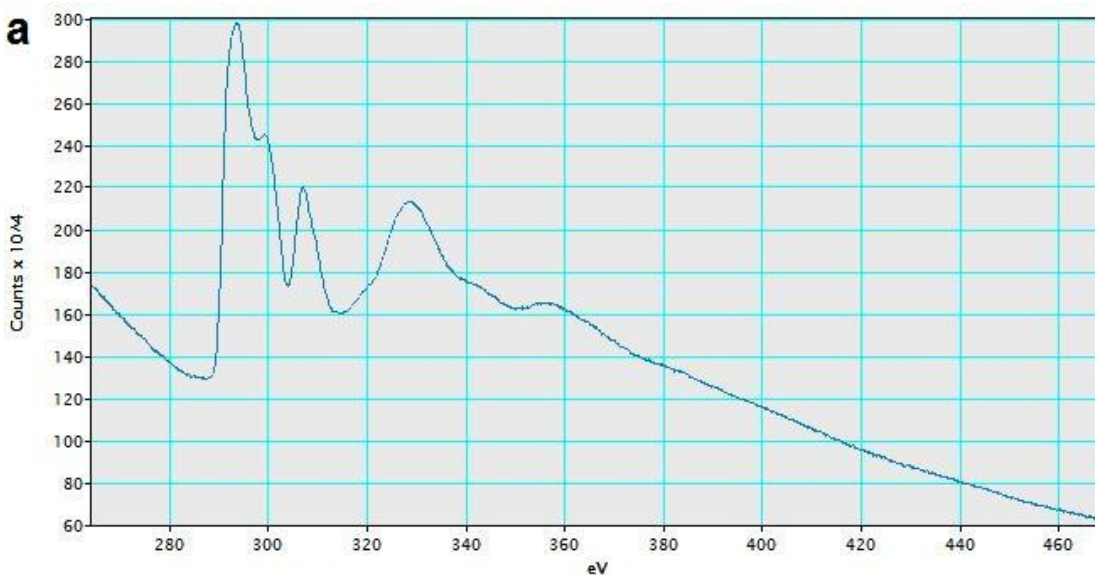


Figure S7: HR-TEM image of UNCD/NCD film synthesized at chamber pressure 100 torr shows differently transformed tiny grains; (1, 4, 6 and 10) grating like shapes, (2 and 12) canals between grating like shapes, (3) tip-to-tip assembling in two grating like shapes, (5, 7, 11 and 13) tiny grains partially transformed into grating like shapes and non-uniform stretching of lattices, (8 and 9) more atoms of tiny grains reveal swelling and in some cases do not form compact configurations and (14) unoccupied space covered the grating like shape; total mass flow rate: 200 sccm (6% H₂, 1 % CH₄ and 93 % argon), microwave power: 1400 watts and deposition time: 60 minutes.



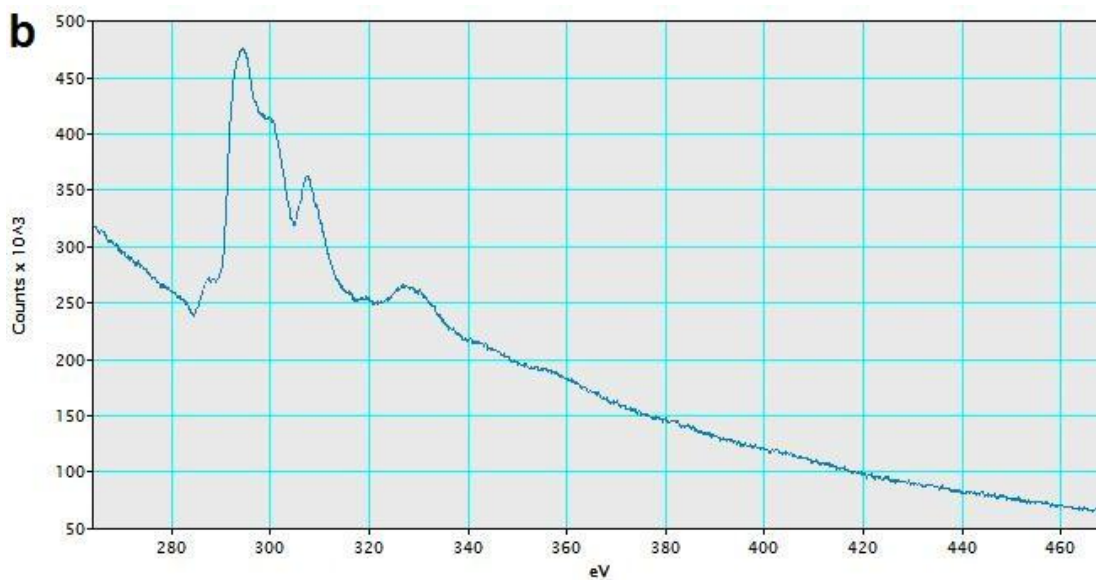
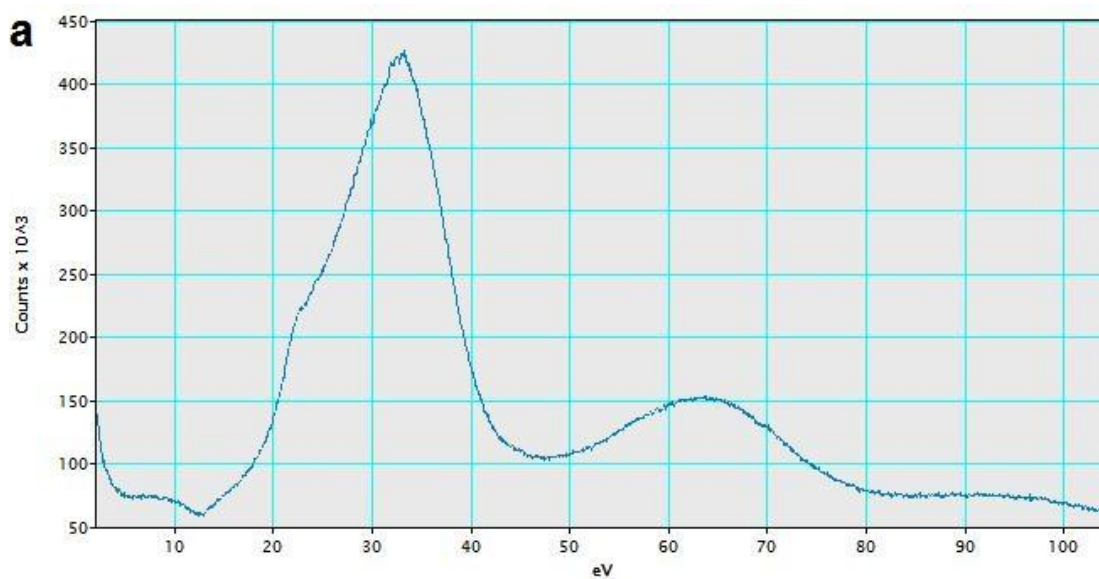


Figure S8: Core Loss EELS of UNCD/NCD films synthesized at chamber pressure (a) 100 torr and (b) 200 torr; total mass flow rate: 200 sccm (6% H₂, 1 % CH₄ and 93 % argon), microwave power: 1400 watts and deposition time: 60 minutes.



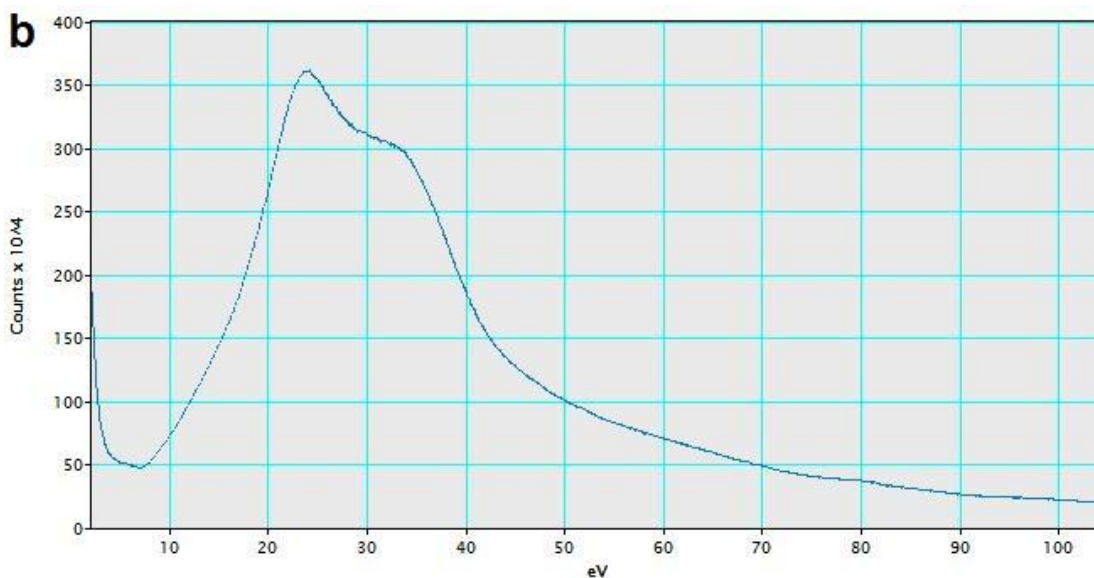


Figure S9: Low loss EELS of UNCD/NCD films synthesized at chamber pressure (a) 100 torr and (b) 200 torr; total mass flow rate: 200 sccm (6% H₂, 1 % CH₄ and 93 % argon), microwave power: 1400 watts and deposition time: 60 minutes.

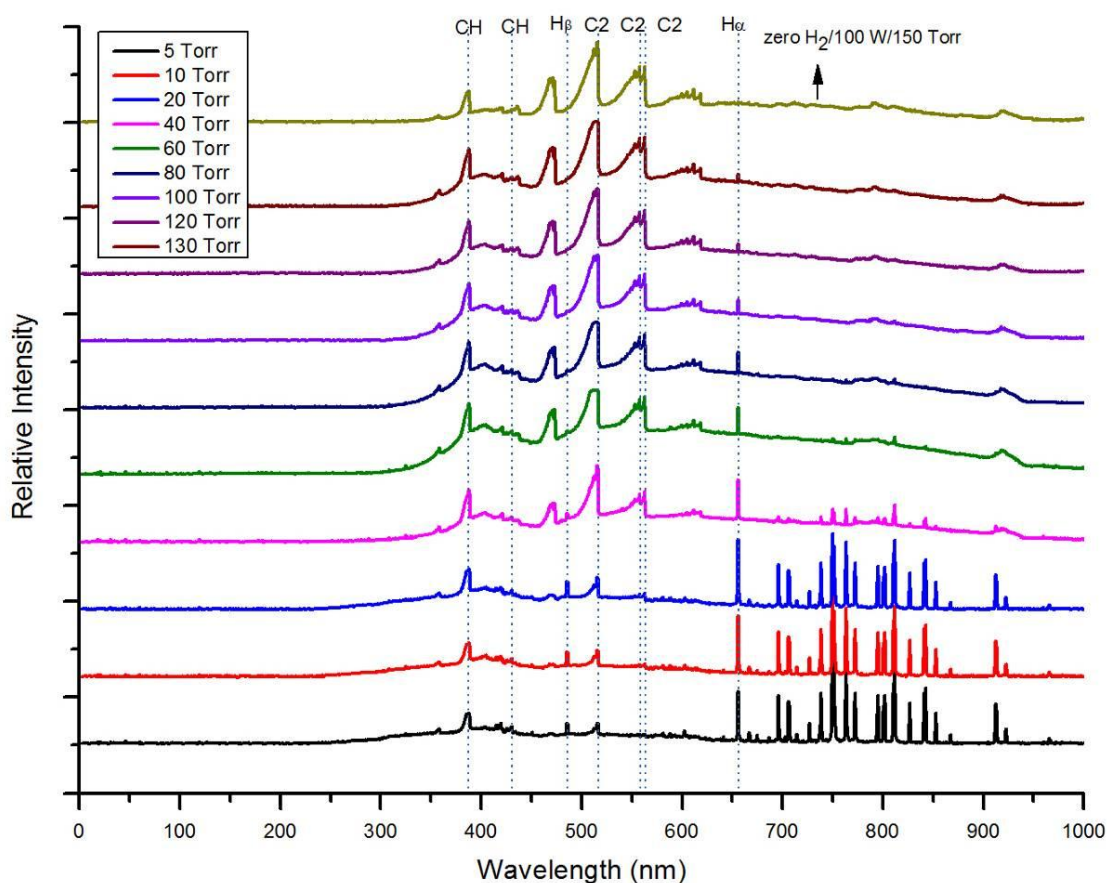


Figure S10: Optical Emission Spectra of the processing plasma at various chamber pressure at total mass flow rate: 200 sccm (3% H₂, 1 % CH₄ and 96 % argon) and microwave power: 1300 watts.